Biophysical Chemistry 16 (1982) 209–221
Elsevier Biomedical Press

JUMPING FREQUENCIES IN MEMBRANE CHANNELS

COMPARISON BETWEEN STOCHASTIC MOLECULAR DYNAMICS SIMULATION AND RATE THEORY

P. LÄUGER and H.-J. APELL

Department of Biology, University of Konstanz, D-7750 Konstanz, F.R.G.

Received 9th March 1982
Accepted 11th June 1982

Key words: Rate theory; Jumping frequency; Membrane channel; Molecular dynamics

Permeation of molecules through membrane channels involves local interactions with a limited number of ligand groups. A method for the molecular dynamics simulation of particle movement in small ligand systems is described. It is assumed that the ligand groups carry out thermal vibrations, whereas the rest of the channel molecule and the surroundings act as a heat bath which is coupled via random forces to the motions of the ligands. The simulation technique is applied to a simple system which contains some of the essential features influencing jumping rates in membrane channels, such as flexibility of ligand configuration or inertial effects in the motion of the ligands. Since the simulation is based on strictly microscopic parameters of the particle-ligand system, a rigorous test of the predictions of rate theory is possible. It is found that rate theory describes the general dependence of jumping frequency k' on temperature and on ligand binding strength rather well, although the values of k' obtained by computer simulation are 2–3 times smaller than those predicted by rate theory.

1. Introduction

The transport of molecules through membrane channels involves a series of thermally activated jumps between sites of low potential energy. The pathway of the permeating particle may thus be represented by a sequence of potential wells separated by activation barriers. The energy wells are the positions where the particle interacts favourably with surrounding ligand groups of the channel molecule, e.g., a protein. In order to estimate the frequency k' of transitions over an energy barrier, rate theory [1] is commonly used in whch k' is represented as the product of the oscillation frequency in the potential well times a Boltzmann factor containing the height of the barrier. In most applications of rate theory to membrane channels, the potential profile has been considered to be fixed, i.e., independent of time and independent of the movement of the permeating particle. In a more realistic approach taking into account thermal movements of the ligand system [2], the static potential is replaced by the so-called potential of mean force [3,4]. Despite this refinement, the application of rate theory still requires certain assumptions to be fulfilled, such as the condition that the ligand system remains in equilibrium even if the particle is driven through the channel by an external force. This means that the use of rate theory becomes questionable in situations where the reorientation time of the ligands is comparable to or longer than the average dwelling time of the particle in the potential well.

An entirely different method for the calculation of transition frequencies is given by molecular dynamics [5–7]. Starting with a set of initial conditions, the coupled Newtonian equations of motion of the molecular system are integrated using a fast digital computer. This method yields the trajectories of the individual atoms of the system from

0301-4622/82/0000–0000/$02.75

which all dynamic parameters of interest such as transition frequencies can be obtained. Molecular dynamics simulations of ion transport in channels can be used as an 'experimental' test of the predictions of rate theory [8]. Simulations for a helical array of 40 dipolar ligand groups have been carried out [8], and the results have been compared with the jumping frequencies calculated on the basis of the ordinary version of rate theory using the static potential.

In the present molecular dynamics study, the properties are analyzed of a ligand system consisting of a mobile particle which interacts with three elastically bound force centers. The rationale behind the study of small ligand systems of this kind is the notion that channels in biological membranes are likely to be constructed in such a way that the permeability is determined by a sort of constriction (sometimes referred to as the 'selectivity filter') where the permeating particle interacts with only a few ligand atoms [9]. The ligand atoms are dynamically coupled to the rest of the channel molecule which acts as a heat bath. In the molecular dynamics simulation which is described in the following, coupling to the heat batch is introduced in the form of random collisions between the ligand atoms and fictitious gas atoms with thermal velocity distribution. This method of stochastic (or Brownian) molecular dynamics [10–14] is particularly suitable for the simulation of small ligand systems. The jumping frequencies determined from the simulation are compared with the predictions of rate theory in the refined version which is based on the potential of mean force.

2. Transport model and equations of motion

We assume that a particle moves along the x-axis and thereby interacts with a ligand which is elastically bound at an equilibrium position b on the y-axis (fig. 1). The interaction of the particle with the central ligand is assumed to be attractive at large distance r and repulsive at small r, such that the motion along the x-axis is restricted by an energy barrier at $x = 0$ (fig. 1). In order to confine the particle to an finite interval on the x-axis, boundary ligands are introduced at positions $-a$ and a. The particle-ligand interactions are described by Lennard-Jones potentials both for the central ligand (parameters ϵ_C and σ_C) and for the boundary ligands (parameters ϵ_B and σ_B). Furthermore, the binding of the central and the boundary ligands to their equilibrium positions is characterized by harmonic force cosntants f_C and f_B, respectively. Neglecting ligand-ligand interactions, the total potential energy of the system is obtained as

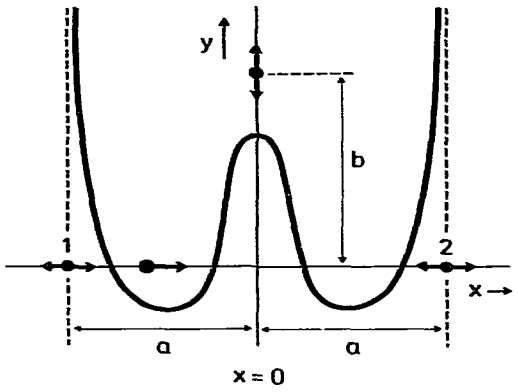

Fig. 1. Transport model for the analysis of jumping frequencies. The particle moves along the x-axis and thereby interacts with a central ligand elastically bound to position b on the y-axis and with boundary ligands 1 and 2 which are bound to positions $-a$ and a on the x-axis. The potential energy of the particle as a function of x is drawn schematically assuming that the interaction with the ligands is attractive at large distance and repulsive at small distance. All ligands experience random collisions with the atoms of a fictitious gas acting as a heat bath.

$$U(x,y,x_1,x_2) = 4\epsilon_B\left[\left(\frac{\sigma_B}{x_1-x}\right)^{12} - \left(\frac{\sigma_B}{x_1-x}\right)^{6} + \left(\frac{\sigma_B}{x_2-x}\right)^{12} - \left(\frac{\sigma_B}{x_2-x}\right)^{6}\right] + 4\epsilon_C\left[\left(\frac{\sigma_C}{r}\right)^{12} - \left(\frac{\sigma_C}{r}\right)^{6}\right] + \frac{f_B}{2}(x_1+a)^2 + \frac{f_B}{2}(x_2-a)^2 + \frac{f_C}{2}(y-b)^2 \quad (1)$$

$$r = \sqrt{x^2+y^2}$$

x_1 and x_2 are the coordinates of the boundary ligands at $x = -a$ and $x = a$, respectively (fig. 1).

For the derivation of the equations of motion

we assume that the total force on the ligands is the sum of a non-statistical force (which is equal to the negative gradient of the potential U) plus a statistical force resulting from the coupling to the heat bath. The particle, on the other hand, is assumed to be coupled to the heat bath only indirectly via the ligands. This corresponds to the situation inside a channel where the permeating particle interacts predominantly with the surrounding ligands which in turn are coupled to the rest of the channel molecule. Denoting the mass of the particle by m_P, the masses of the central and boundary ligands by m_C and m_B, respectively, the equations of motion are obtained in the form

$$m_P \ddot{x} = -\frac{\partial U}{\partial x} \tag{2}$$

$$m_C \ddot{y} = -\frac{\partial U}{\partial y} + K_{C,stat} \tag{3}$$

$$m_B \ddot{x}_1 = -\frac{\partial U}{\partial x_1} + K_{1,stat} \tag{4}$$

$$m_B \ddot{x}_2 = -\frac{\partial U}{\partial x_2} + K_{2,stat} \tag{5}$$

For the calculation of the statistical forces $K_{C,stat}$, $K_{1,stat}$ and $K_{2,stat}$ the following stochastic model is used. It is assumed that the ligand atoms move in a gas with thermal velocity distribution and experience random collisions with the gas atoms. This model accounts in an approximate way for the stochastic forces exerted on the ligands by neighbouring atoms of the channel molecule and ensures that the velocity of the ligand atoms is randomized. For the determination of the statistical force K_{stat}, the time t is subdivided into intervals of length Δt_c and a decision is made for each interval (using a random number generator) whether a collision occurs during Δt_c (see Appendix A). If the decision is positive, a value p of the momentum transmitted to the ligand is selected at random from the interval $(-p_{max}, p_{max})$ with the probability distribution

$$h(p) = \frac{|p|}{p_{max}} \exp\left[-\frac{m_H}{2kT}(v + p/2\mu)^2\right] \tag{6}$$

(Appendix A), where k is Boltzmann's constant, T the absolute temperature, m_H the mass of a gas atom in the heat bath, $\mu = m_H m/(m_H + m)$ the reduced mass and v the velocity of the ligand. $p_{max} > 0$ is an upper limit of the transmitted momentum which has been chosen such that values of p larger than p_{max} are rare (see Appendix A). From the selected value of p the average statistical force acting on the ligand during the collision interval Δt_c is obtained as

$$K_{stat} = \frac{p}{\Delta t_c} \tag{7}$$

3. Transition frequency predicted by rate theory

In the traditional version of rate theory [1,3] the jumping frequency k' over a barrier from left to right may be approximated by the relation

$$k' = \nu \cdot \exp(-E/kT) \tag{8}$$

where ν is the oscillation frequency of the particle in the energy well to the left of the barrier and E the energy difference between the top of the barrier and the well. Eq. 8 describes situations where the potential energy profile can be assumed to be a time-independent property of the system. In order to apply rate theory to flexible ligand systems exhibiting fluctuations of barrier height, the ordinary potential function has to be replaced by the potential of mean force [3,4,16]. Starting with the total potential $U(x, y, x_1, x_2)$ as given by eq. 1, the configuration integral $Q(x)$ of the ligand system with the particle positioned at x is defined by

$$Q(x) = \iiint \exp[-U(x, y, x_1, x_2)/kT]\, dy dx_1 dx_2 \tag{9}$$

The potential $V(x)$ of mean force is then obtained as [3,4]:

$$V(x) = -kT \ln \frac{Q(x)}{Q(\infty)} \tag{10}$$

The quantity $Q(\infty)$ which serves as a normalization constant is the configuration integral of the ligand system without a particle. The potential of mean force represents an average over all thermally accessible ligand positions and therefore accounts for the flexibility of the ligand system. As shown in Appendix B, the transition frequency over the barrier may be obtained from $V(x)$ according to

$$k' = \sqrt{\frac{2kT}{\pi m_P}} \cdot \frac{\exp[-V(0)/kT]}{\int_{-a}^{a} \exp[-V(x)/kT]\, dx} \tag{11}$$

4. Results

The Lennard-Jones parameters of eq. 1 for the interaction between particle and ligands were chosen to be the same as those for the interaction between argon atoms: $\epsilon_B/k = \epsilon_C/k \simeq 125$ K, $\sigma_B = \sigma_C = 0.34$ nm [18]. For the resting positions the values $a = 0.51$ nm and $b = 0.297$ nm were adopted throughout. In thermal equilibrium with the surroundings the ligands carry out random oscillations about these resting positions with (relative) mean thermal amplitudes

$$\alpha_B \equiv \frac{1}{a}\sqrt{\overline{(x_i - a)^2}} = \frac{1}{a}\sqrt{\frac{kT}{f_B}} \qquad (12)$$

$$\alpha_C \equiv \frac{1}{b}\sqrt{\overline{(y - b)^2}} = \frac{1}{b}\sqrt{\frac{kT}{f_C}} \qquad (13)$$

($i = 1, 2$). The force constant f of eq. 1 was chosen such that the thermal oscillation amplitude of the outer ligands was $\alpha_B = 0.05$ at $T = 300$ K ($f_B \simeq$ 6.4 J m^{-2}) whereas f_C was varied to give oscillation amplitudes α_C of the central ligand between 0 and about 0.3.

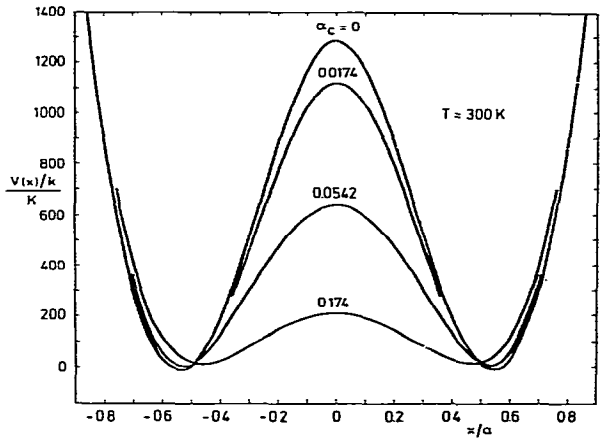

Fig. 2. Potential $V(x)$ of mean force of the particle as a function of position x for different values of the mean thermal amplitude α_C of the central ligand. α_C is varied at constant temperature T by varying the force constant f_C of the ligand (eq. 13). The ratio $V(x)/k$ is given in kelvin (k is Boltzmann's constant). $\epsilon_B/k = \epsilon_C/k = 125$ K, $\sigma_B = \sigma_C = 0.34$ nm, $a = 0.51$ nm, $b = 0.297$ nm, $\alpha_B = 0.05$, $T = 300$ K. $V(x)$ was calculated according to eqs. 9 and 10 using a 20-point Gauss-Hermite formula for the numerical approximation of the multiple integral in eq. 9 [4,19]. The zero point of $V(x)$ corresponds to infinite distance of the particle from the ligand system.

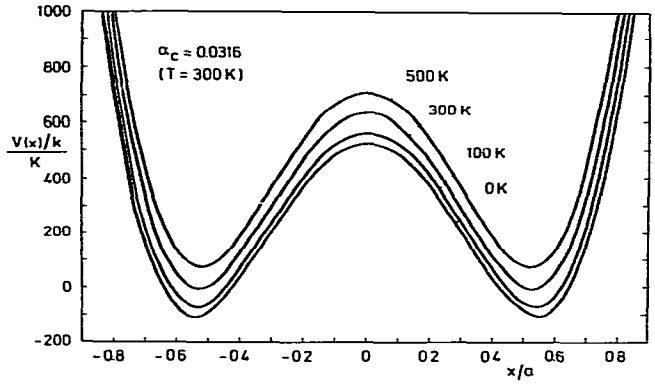

Fig. 3. Potential $V(x)$ of mean force for different temperatures T. The force constants of ligand binding were chosen such tat the mean thermal oscillation amplitudes were $\alpha_B = 0.05$ and $\alpha_C = 0.0542$ at $T = 300$ K; all other parameters had the values given in the legend to fig. 2. The zero point of $V(x)$ refers to infinite distance of the particle from the ligand system. The potential for $T = 0$ which is identical with the adiabatic potential of the particle was calculated in the following way [8]. For each fixed position x of the particle, the equations of motion were integrated starting with all ligand atoms at rest in their initial equilibrium positions $x_1 = -a$, $x_2 = a$, $y = b$. In order to achieve an asymptotic approach to the new equilibrium positions $\bar{x}_1$, $\bar{x}_2$, $\bar{y}$, friction terms proportional to negative velocity were added to the total force. The adiabatic potential was then obtained by inserting $\bar{x}_1$, $\bar{x}_2$ and $\bar{y}$ into eq. 1.

The profile of the potential $V(x)$ of mean force (eq. 10) is represented in fig. 2 for different values of α_C. The central barrier is highest for a fixed ligand ($\alpha_C = 0$) and becomes gradually lower as the binding of the ligand becomes weaker. This means that the jumping frequency over the barrier should depend on the flexibility of the ligand system.

Potential profiles for different temperatures are shown in fig. 3. The temperature dependence of $V(x)$ results from the fact that the potential of mean force which has the character of a free energy represents an average over the thermally accessible ligand configurations. It is seen that $V(x)$ is shifted upward with increasing temperature. This is consistent with expectation, since the

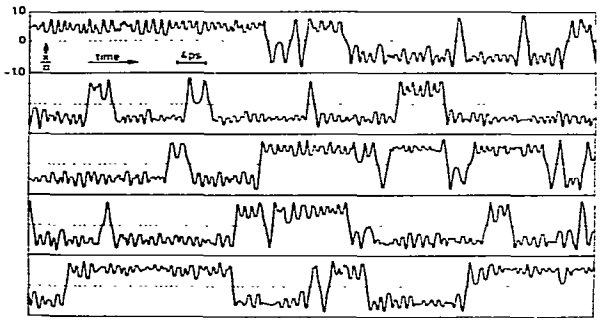

Fig. 4. Trajectory of the particle under the condition of equal mass of particle and central ligand ($m_P = m_C = m_H = 6.6 \times 10^{-23}$ g). The coordinate x of the particle is given in units of x/a with $a = 0.51$ nm, $b = 0.297$ nm, $\epsilon_B/k = \epsilon_C/k = 125$ K, $\sigma_B = \sigma_C = 0.34$ nm, $\alpha_B = 0.05$, $\alpha_C = 0.0542$, $m_B = m_H = 6.6 \times 10^{-23}$ g, $T = 300$ K, $\Delta t = 0.002$ ps, $\lambda_B = \lambda_C = 20$, $\nu_B^0 = \nu_C^0 = 2.5$ ps^{-1} (λ is the number of integration time steps per collision interval (eq. C1) and ν^0 the average frequency of collisions with the ligand at rest (eq. A5); B and C refer to the boundary ligands and the central ligand, respectively).

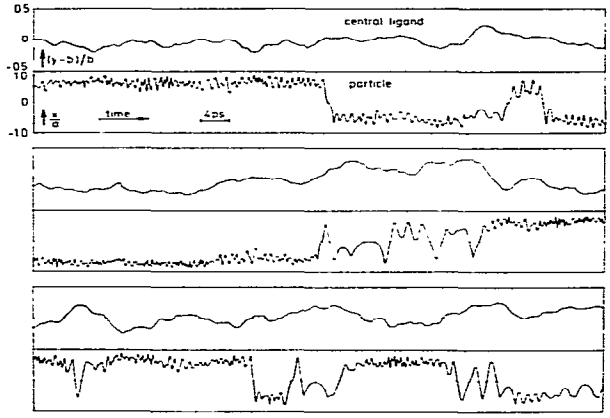

Fig. 5. Simultaneously recorded trajectories of central ligand and particle under the condition of tight coupling of the central ligand to a massive domain of the transport protein. Both the mass of the ligand ($m_C = 200 m_H = 1.32 \times 10^{-20}$ g) and the frequency of collisions ($\nu_C^0 = 75$ ps^{-1}) have been chosen to be much larger than those in fig. 4, whereas the force constant was reduced to yield a relative thermal amplitude of $\alpha_C = 0.343$. $m_B = 2 m_H = 1.32 \times 10^{-22}$ g, $\lambda_C = 1$; all other parameters had the same values as in fig. 4.

restriction of thermal motions of the ligands by the particle makes an unfavourable contribution to the free energy of the system. The potential profile for $T = 0$ is identical with the so-called adiabatic potential [8], i.e., the potential corresponding to the situation where the particle is moved slowly along the x-axis and the ligands are allowed to assume their resting positions.

For the molecular dynamics simulation, both the mass m_P of the particle and the mass m_H of the gas atoms representing the heat bath were set equal to the mass of the argon atom ($m_P = m_H = 6.6 \times 10^{-23}$ g), if not otherwise indicated. The mass of a boundary ligand atom was usually chosen to be twice as large ($m_B = 2 m_H$), whereas the mass of the central ligand was varied between m_H and $200 m_H$. Approximate time scales of the motions are then given by the intrinsic oscillation period of the boundary ligands: $\tau = 2\pi\sqrt{m_B/f_B} \simeq 0.91$ ps (with $f_B = 6.4$ J m^{-2}), and by the 'flight time' of a free particle of mass m_P moving a distance a with mean thermal velocity: $\tau_0 = a\sqrt{m_P/kT} \simeq 2.0$ ps (at $T = 300$ K). For the numerical integration of the equations of motion (Appendix C) a time step of $\Delta t = \tau_0/1000 = 0.002$ ps was used in most cases; it was verified that further reduction of Δt did not change the results significantly.

In order to check the effectiveness of coupling of the system to the heat bath, the average kinetic energy E_{kin} of the ligands and the particle was calculated by taking values of the kinetic energy every 0.2 ps (the total duration of the simulation was usually about 1 ns). E_{kin} was found to agree with $kT/2$ in most cases within 10%.

An example of a trajectory of the particle under the condition of equal mass of particle and central ligand is represented in fig. 4. The particle oscillates over extended periods of time in either the left-hand or right-hand energy well, and occasionally jumps over the barrier. It is also apparent from fig. 4 that jumps frequently occur in pairs. Such double (or multiple) transitions are favoured by the correlation of the motions of ligand and particle (see below) and furthermore by the fact that the particle, once it has gained a high kinetic energy, will lose this energy (on the average) only after some further collisions.

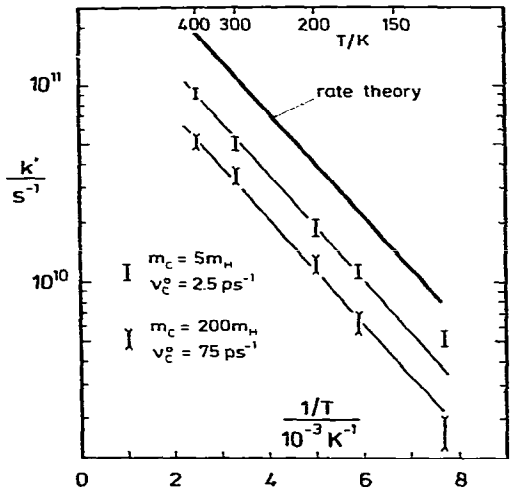

Fig. 6. Jumping frequency k' over the barrier from left to right as a function of reciprocal temperature. The upper curve represents the values of k' as predicted by rate theory (eq. 11). The integral in eq. 11 was calculated using a mixed 20-point Gauss-Hermite-Legendre formula [4,19]. Results of molecular dynamics simulations are given for a weakly damped central ligand (middle curve, $m_C = 5m_H$, $\nu_C^0 = 2.5\ ps^{-1}$) and for a massive, strongly damped central ligand (lower curve, $m_C = 200m_H$, $\nu_C^0 = 75\ ps^{-1}$). $m_P = m_H = 6.6 \times 10^{-23}$ g, $m_B = 2m_H$, $\alpha_C = 0.0542$ (at 300 K), $\lambda_B = 20$ (middle curve) or 1 (lower curve), $\Delta t = 0.002$ ps; all other parameters had the same values as in fig. 2. The length of the simulation period varied between 1 and 4 ns. Error limits were estimated according to eq. 14; it should be noted that eq. 14 tends to underestimate the statistical error (see text). From the slope of the straight lines an activation energy $E_A = -R \cdot d \ln k'/d(1/T) \approx 5.10$ kJ mol^{-1} is obtained (R is the gas constant).

In the second example shown in fig. 5 it has been assumed that the central ligand is tightly coupled to an entire domain of the transport protein. Since the motion of a massive domain is governed by a large number of (weak) interactions with the surroundings, the frequency of collisions ($\nu_C^0 = 75\ ps^{-1}$) has been considerably increased in comparison with the previous example. The mass m_C of the ligand has been set equal to 200 m_H and the force constant has been reduced, yielding a relative thermal amplitude of $\alpha_C = 0.343$. In fig. 5 the trajectories of the central ligand and of the particle are represented simultaneously. It is seen that in this case the ligand behaves as a strongly damped Brownian oscillator. This is in contrast to the previous example where the trajectory of the central ligand (not shown) exhibits a more regular (pseudo-periodic) behaviour. The diffusive nature of the massive ligand in fig. 5 results from the high frequency of collisions with the atoms of the surroundings which corresponds to an increased friction. An interesting finding which is apparent from fig. 5 is the correlation of the motions of the central ligand and the particle. During time periods where the ligand is farther apart from the x-axis (corresponding to positive values of $(y - b)$) there is an increased probability of the particle jumping to the other side. Since for positive values of $(y - b)$ the repulsive interaction between ligand and particle is reduced, this means that transitions mainly occur when the barrier is low.

Values of the rate constant k' have been determined from extended simulation periods (usually 1–3 ns). If totally z jumps have been recorded during the simulation time t_s, the rate constant is obtained as $k' = z/2t_s$, since half of the jumps are directed from left to right. k' is represented in fig. 6 for different temperatures and for the two situations already illustrated in figs. 4 and 5, i.e., weak and strong damping of the central ligand. In both cases the temperature dependence of k' agrees with the predictions of rate theory (uppermost curve), but the absolute values of k' as obtained from the simulation are lower by a factor of about 2.1 (weak damping) and 3.5 (strong damping).

For an estimate of the statistical error involved in the determination of k' the following model was used [8]. If the particle oscillates with frequency ν in the potential, it makes νt_s attempts to cross the barrier during the simulation time t_s, out of which z are successful. The error Δz may be defined as the square root of the variance of the corresponding binomial distribution:

$$\Delta z \equiv \sqrt{\overline{(z - \bar{z})^2}} = \sqrt{\bar{z}(1 - \bar{z}/\nu t_s)} \approx \sqrt{z(1 - z/\nu t_s)} \qquad (14)$$

The average oscillation frequency ν which enters into eq. 14 may be obtained from the trajectory or from the shape of the potential function $V(x)$ using the approximate relation $2\pi\nu = \sqrt{V''/m_P}$, where V'' is the second derivative of $V(x)$ at the

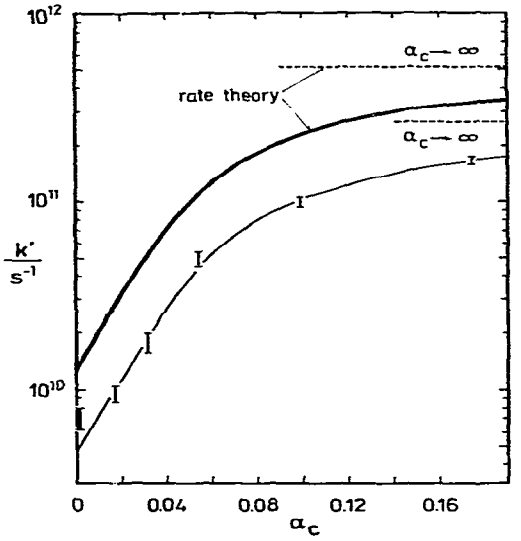

Fig. 7. Jumping frequency k' as a function of mean thermal vibration amplitude α_C of the central ligand. The upper curve represents the values of k' as predicted by rate theory (eq. 11). The molecular dynamics simulation (lower curve) has been carried out with $m_P = m_B = m_H = 6.6 \times 10^{-23}$ g, $m_C = 10 m_H$, $\nu_B^0 = \nu_C^0 = 2.5$ ps^{-1}, $\lambda_B = \lambda_C = 20$, $\Delta t = 0.002$ ps; all other parameters had the same values as in fig. 2. The length of the simulation period varied between 1 and 4 ns. The dashed lines represent the limiting values of k' in the absence of a central barrier ($\alpha_C \to \infty$ or $\epsilon_C = 0$).

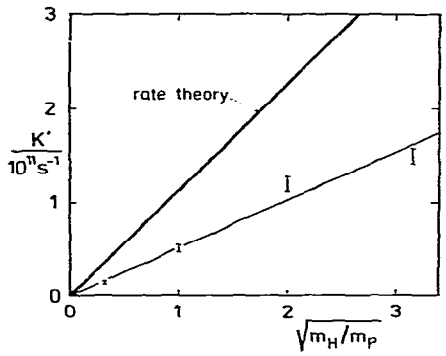

Fig. 8. Effect of particle mass m_P on jumping frequency k'. m_P is given by the dimensionless ratio m_P/m_H, where $m_H = 6.6 \times 10^{-23}$ g is a reference mass. $m_B = 2m_H$, $m_C = 5m_C$, $\alpha_C = 0.0316$, $\lambda_B = \lambda_C = 20$, $\nu_B^0 = \nu_C^0 = 2.5$ ps^{-1}; all other parameters had the same values as in fig. 2. The upper curve represents the jumping frequency as predicted by rate theory (eq. 11).

location of the well. The calculation of Δz (and of $\Delta k' = \Delta z / 2 t_s$) from eq. 14 tends to underestimate the error, since correlations between successive jumps are neglected.

In order to study the influence of flexibility of the ligand system on the jumping rates, the force constant of the central ligand was varied. The dependence of k' on the mean thermal vibration amplitude α_C of the central ligand is shown in fig. 7. As may be expected from the predominantly repulsive interaction between particle and ligand, the transition rate constant is small for a rigid ligand ($\alpha_C = 0$) and increases with increasing α_C. Rate theory and molecular dynamics simulation agree in the general form of the dependency of k' on α_C, but again the values of k' obtained from the simulation are lower by a factor of 2.0 – 2.8 in the range of α_C studied.

According to eq. 11, rate theory predicts that the rate constant k' should be inversely proportional to the square root of particle mass m_P (this relationship between k' and m_P is implicitly contained also in the simplified rate-theory equation (eq. 8), since $\nu \propto 1/\sqrt{m_P}$). As fig. 8 shows, the values of k' as obtained from the simulation are indeed proportional to $1/\sqrt{m_P}$, but with a lower proportionality factor than predicted.

From eq. 11 it may further be expected that k' is insensitive to a change of ligand mass. In order

Table 1

Jumping frequency k' as a function of the mass m_C of the central ligand for two different values of the mean thermal amplitude α_C

$m_B = m_P = m_H = 6.6 \times 10^{-23}$ g, $\lambda_B = \lambda_C = 20$, $\nu_B^0 = \nu_C^0 = 2.5$ ps^{-1}; all other parameters had the same values as in fig. 2. The error limits have been estimated according to eq. 14.

α_C	$\frac{m_C}{m_H}$	$k' \, 10^{11} \, s^{-1}$
0.0542	1	0.485 ± 0.044
	10	0.494 ± 0.044
	100	0.448 ± 0.037
0.171	1	1.65 ± 0.06
	10	1.67 ± 0.06
	100	1.52 ± 0.07

to test this prediction, m_C was varied in the range 1–100 for two different values of α_C. As may be seen from Table 1, the jumping frequency k' is virtually independent of m_C.

A further series of simulations was carried out to study the effect of damping of ligand motion on the transition rate constant. As shown in Appendix A, the damping, say, of the central ligand may be described by a friction coefficient $\beta_C = 4\mu_C \nu_C^0$ where $\mu_C \equiv m_C m_H/(m_C + m_H)$ is the reduced mass and ν_C^0 the collision frequency of gas atoms of the heat bath with the ligand. The motion becomes overdamped when $\beta_C > \beta_{C,crit} = 2\sqrt{f_C m_C}$. The collision frequency $\nu_C^0 = \nu_B^0$ was varied between 0.5 and 150 ps^{-1} under the conditions $\alpha_B = \alpha_C = 0.05$, $m_B = m_P = m_H$, $m_C = 10 m_H$; this means that at the upper limit of ν_C^0 the friction coefficient was $4.7 \times \beta_{C,crit}$. The transition frequency k' was found to be the same within the limits of statistical error in the whole range in which β_C and β_B were varied. This result may be compared with the observation of Beece et al. [26] that the diffusive motion of carbon monoxide in the interior of a myoglobin molecule depends only weakly on the viscosity of the surrounding medium. The finding that k' is rather insensitive to the mass and the friction coefficient of the central ligand is already contained in fig. 6. (The reduction of k' in the case of the massive ligand possibly results from the combination of large mass and strong damping).

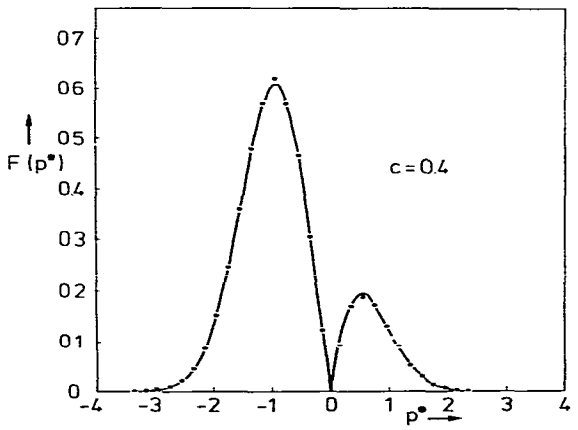

Fig. 9. Probability distribution of momenta p transmitted on a ligand atom moving with velocity $v = 0.4\sqrt{m_H/2kT}$ in a medium of gas atoms of mass m_H. The momentum is expressed as a dimensionless quantity $p^* = p\sqrt{m_H \mu^2 kT}$, where μ is the reduced mass of the colliding pair. The points have been obtained by the random number method described in the text using eq. C2 with $c = 0.4$ and $p^*_{max} = 5$: they represent the probability density $N(p^*)/N\Delta p^*$, where $N = 2 \times 10^5$ is the total number of transmitted momenta and $N(p^*)$ the number of momenta lying in an interval $\Delta p^* = 0.1$ around p^*. The line represents the theoretically expected probability density $F(p^*)$ (eq. C3).

5. Discussion

In this study we have described a method for the dynamic analysis of particle movement in small ligand systems. This method can serve for an approximate treatment of transport through membrane channels in which the motion of the permeating molecule is governed by local interactions with a limited number of ligand atoms. The molecular dynamics method applied here is based on the assumption that the rest of the channel molecule and the surroundings can be treated simply as a heat bath which is coupled via random forces to the ligands. In order to introduce random forces into the equations of motion the Langevin formalism has been mainly used in the past which requires the definition of a friction coefficient [11–14,22–25]. In the method described here we have avoided phenomenological quantities such as friction coefficients, since the meaning of a friction coefficient describing motion in a protein channel seems obscure [16]. Instead, we have based the statistics of momentum exchange between ligands and heat bath on a strictly microscopic model in which the heat bath is represented by a gas with a Maxwell-Boltzmann velocity distribution. Similar procedures have been applied by others to problems involving rotational motion and isomerization dynamics in condensed phases [10,21]. In these previous studies, however, it was assumed that the velocities become completely randomized at each collision, whereas in the method used here the form of momentum exchange in a head-on collision between gas atom and ligand is taken into account explicitly. Accordingly, it is possible to correlate a posteriori a formal friction coeffi-

cient with the parameters of the statistical model, i.e., the average collision frequencies and the masses of the gas atom and of the ligand (see Appendix A).

The main purpose of the molecular dynamics simulations described here was a test of the predictions of rate theory for a simple system which nevertheless contains some of the essential elements influencing jumping rates in membrane channels, such as flexibility of ligand configuration or inertial effects due to the atomic masses of the ligand groups. A rigorous test of rate theory (as applied to membrane channels) is difficult to carry out experimentally, since this would require a knowledge of both the jumping rate constant k' and the exact form of $V(x)$ in eq. 11. In a computer simulation, however, k' is an 'experimental' quantity and $V(x)$ can be separately calculated from the microscopic parameters of the model. It was found that rate theory did describe the general dependence of k' on temperature and on the binding strength of the central ligand rather well, although the predicted values were larger by a factor of 2.1–3.5 than the results of the computer simulation (figs. 6 and 7). It should be emphasized, however, that eq. 11 represents a refined form of rate theory which is based on the potential $V(x)$ of mean force accounting for thermal fluctuations in ligand geometry. Much larger discrepancies between rate theory and molecular dynamics simulation would have been observed if the potential function of the rigid ligand system (with the ligands fixed in their equilibrium positions) had been used.

From the temperature dependence of k' (fig. 6), an activation energy $E_A = -R \cdot \mathrm{d} \ln k'/\mathrm{d}(1/T) = 5.10$ kJ/mol is obtained which corresponds to $E_A/R = 614$ K (R is the gas constant). This value is close to the barrier height $E/k = 640$ K determined from the potential of mean force (fig. 3, $T = 300$ K). In the system studied here the activation energy also approximately agrees with the barrier height determined from the adiabatic potential (fig. 3, 0 K) which is about 625 K. This agreement, however, is not generally observed; for instance, in a system with strong coulombic interaction a large discrepancy between adiabatic potential and activation energy from molecular dynamics simulation was found [8].

Two other predictions of rate theory are borne out by molecular dynamics simulation: the jumping frequency k' is inversely proportional to the square root of particle mass m_P (fig. 8), and k' is virtually insensitive to a variation of ligand mass m_C (table 1). It may be expected, however, that in other systems effects of ligand mass on k' do occur, since the dynamic coupling between ligand and particle depends on the geometry and on the nature of the ligand-particle interactions.

Acknowledgements

The authors wish to thank Dr. J. Brickmann, Dr. H. Schröder and W. Fischer for interesting discussions. This work has been financially supported by Deutsche Forschungsgemeinschaft (Sonderforschungsbereich 138).

Appendix A

A.1. Calculation of the statistical forces

We assume that a ligand atom of mass m moves along a given direction and experiences random head-on collisions with surrounding gas atoms of mass m_H. In thermal equilibrium the probability density $f(v_H)$ for the velocity v_H of a gas atom in direction of the y-axis is given by a Maxwell distribution [15]:

$$f(v_H) = \sqrt{\frac{m_H}{2\pi kT}} \cdot \exp\left(-\frac{m_H v_H^2}{2kT}\right) \tag{A1}$$

where k is Boltzmann's constant and T the absolute temperature. If v is the velocity of the ligand atom, the relative velocity v_r of the gas atom with respect to the ligand is given by

$$v_r = v_H - v \tag{A2}$$

Introducing the number n of gas atoms per unit volume and the collision cross-section s, the frequency $\mathrm{d}\nu$ of collisions of a ligand atom in the velocity interval $(v_r, v_r + \mathrm{d}v_r)$ is obtained as

$$\mathrm{d}\nu = ns|v_r| f(v_H)\, \mathrm{d}v_r \tag{A3}$$

By integration of eq. A3 between $v_r = -\infty$ and

$v_r = \infty$ the total mean frequency ν of collisions is obtained ($c \equiv v\sqrt{m_H/2kT}$):

$$\nu = \nu^0[\sqrt{\pi}c\Phi(c) + \exp(-c^2)] \tag{A4}$$

ν^0 is the collision frequency with the ligand at rest ($v = 0$):

$$\nu^0 = ns\sqrt{\frac{2kT}{\pi m_H}}\,. \tag{A5}$$

and $\Phi(x)$ is the error function:

$$\Phi(x) = \frac{2}{\sqrt{\pi}}\int_0^x \exp(-u^2)\,du$$

During the collision the momentum of the ligand atom is changed by an amount p which is given by

$$p = \frac{2m_H m}{m_H + m}v_r = 2\mu v_r \tag{A6}$$

where μ is the reduced mass. Combining eqs. A1–A6 yields the frequency of collisions during which a momentum in the interval (p, $p + dp$) is transmitted to the ligand:

$$d\nu = \frac{\nu^0 m_H}{8kT\mu^2}|p|\exp\left[-\frac{m_H}{2kT}(v + p/2\mu)^2\right]dp \tag{A7}$$

It is seen from eq. A7 that the probability distribution for the transfer of a momentum of magnitude p depends on v and is asymmetric with respect to $p = 0$, as expected. A momentum change by which the ligand velocity is diminished (p and v having opposite signs) always occurs with higher likelihood. This property of the probability distribution corresponds to a friction effect of the surrounding gas on the ligand (see below).

The time t is subdivided into intervals of length Δt_c, and in the course of the integration a decision is made for each time interval (using a random number generator) whether a collision occurs during Δt_c. The collision probability is set equal to $\nu\Delta t_c$, where ν is calculated from eq. A4 with the instantaneous value of v (Δt_c is chosen such that always $\nu\Delta t_c \ll 1$). If a collision occurs, the momentum of the ligand is changed by an amount p which is selected at random from an interval ($-p_{max}$, p_{max}) with the probability distribution:

$$h(p) = \frac{|p|}{p_{max}}\exp\left[-\frac{m_H}{2kT}(v + p/2\mu)^2\right] \tag{A8}$$

(cf. eq. A7). $p_{max} > 0$ is an upper limit of the momentum which in practice may be chosen to be $10 \times p_{th} \equiv 2\mu v_{th}$, where $v_{th} = \frac{1}{2}(\sqrt{kT/m_H} + \sqrt{kT/m}$ is the mean of the thermal velocities of gas atom and ligand. From the selected value of p, the average statistical force acting on the ligand during the collision interval Δt_c is obtained as

$$K_{stat} = \frac{p}{\Delta t_c} \tag{A9}$$

The parameters of the statistical model may be correlated with the friction coefficient β describing the average force $\bar{K}$, acting on a ligand atom which is moved with constant velocity v through the gas:

$$\bar{K} = -\beta v \tag{A10}$$

$\bar{K}$ is the total momentum transmitted to the ligand per unit time:

$$\bar{K} = \int 2\mu v_r dv = 2\mu ns\int_{-\infty}^{\infty} v_r|v_r|f(v_H)dv_r \tag{A11}$$

Introduction of eq. A1 and integration yields

$$\bar{K} = -2\mu ns\frac{kT}{m_H}\left[(1 + 2c^2)\Phi(c) + \frac{2c}{\sqrt{\pi}}\exp(-c^2)\right] \tag{A12}$$

($c \equiv v\sqrt{m_H/2kT}$). In the limit of small velocities ($c \ll 1$) the approximation $\Phi(c) \approx 2c/\sqrt{\pi}$ holds. This gives, together with eqs. A10 and A5:

$$\beta = 4\mu ns\sqrt{\frac{2kT}{\pi m_H}} = 4\mu\nu^0 \tag{A13}$$

At low β the ligand exhibits quasi-periodic and at high β diffusive motion, the limit between the two regimes being given by the condition of critical damping:

$$\beta_{crit} = 4\mu\nu^0_{crit} = 2\sqrt{fm} \tag{A14}$$

(f is the force constant of ligand binding). Finally, from β the velocity correlation time $\tau_v = m/\beta$ of the ligand is obtained as

$$\tau_v = \frac{1 + m/m_H}{4\nu^0} \tag{A15}$$

Appendix B

B.1. Derivation of eq. 11

We consider a large number N of identical ligand systems (fig. 1), each containing a particle

of mass m_P located on the x-axis somewhere between $-a$ and a. The Hamiltonian $\mathcal{H}$ of the ligand system depends on the coordinates x, y, x_1, x_2 via the potential energy U, and on the momenta p_x, p_y, p_{x1}, p_{x2}:

$$\mathcal{H} = U(x, y, x_1, x_2) + \frac{p_x^2}{2m_P} + \frac{p_y^2}{2m_C} + \frac{p_{x1}^2}{2m_B} + \frac{p_{x2}^2}{2m_B} \quad \text{(B1)}$$

Under equilibrium conditions, the average number dN of systems in the interval (x, $x + dx$; ...; p_{x2}, $p_{x2} + dp_{x2}$) of phase space is given by

$$dN = N \cdot f(x, \ldots, p_{x2}) dx \ldots dp_{x2} \quad \text{(B2)}$$

The distribution function f is connected with the Hamiltonian by the statistical-mechanical relation [17]

$$f = \frac{\exp(-\mathcal{H}/kT)}{Z} \quad \text{(B3)}$$

where Z is the (classical) partition function:

$$Z = \int \ldots \int \exp(-\mathcal{H}/kT) dx \ldots dp_{x2} \quad \text{(B4)}$$

The integration interval for the x-coordinate is $(-a, a)$ and for the other coordinates $(-\infty, \infty)$. Introducing the configuration integral $Q(x)$ as defined by eq. 9, the partition function becomes

$$Z = (2\mu kT)^2 m_B \sqrt{m_P m_C} \int_{-a}^{a} Q(x) dx \quad \text{(B5)}$$

In the ensemble of N channels, ϕ' transitions take place per unit time over the barrier at $x = 0$ from left to right. If $d\phi'$ is the contribution of all systems in the interval (y, $y + dy$; ...; p_{x2}, $p_{x2} + dp_{x2}$) to the particle flux ϕ' over the barrier, then

$$d\phi' = \left(\frac{dN}{dx}\right)_{x=0} \cdot \frac{p_x}{m_P} \quad (p_x > 0) \quad \text{(B6)}$$

Eq. B6 expresses the fact that the flux from left to right is equal to the density dN/dx of systems times the velocity $v_x = p_x/m_P$ in the direction of the positive x-axis. After introduction of eq. B2 into eq. B6, the total flux is obtained as

$$\phi' = N \int \ldots \int \frac{p_x}{m_P} f(0, y, \ldots, p_{x2}) \, dy dx_1 dx_2 dp_x \ldots dp_{x2} \quad \text{(B7)}$$

Using the relation

$$\int_0^\infty \frac{p_x}{m_P} \exp(-p_x^2/2m_P kT) dp_x = kT \quad \text{(B8)}$$

as well as eqs. B3 and B5, the result is obtained as

$$\phi' = N \sqrt{\frac{kT}{2\pi m_P}} \cdot \frac{Q(0)}{\int_{-a}^{a} Q(x) dx} \quad \text{(B9)}$$

Since $N/2$ is the average number of ligand systems having a particle located on the left side of the barrier, the relation

$$\phi' = \frac{N}{2} k' \quad \text{(B10)}$$

holds, where k' is the rate constant of jumps from left to right. Comparison with eq. B9 and introduction of the potential of mean force from eq. 10 finally yields

$$k' = \sqrt{\frac{2kT}{\pi m_P}} \cdot \frac{\exp[-V(0)/kT]}{\int_{-a}^{a} \exp[-V(x)/kT] dx} \quad \text{(B11)}$$

Appendix C

C.1. Simulation technique

The equations of motion were integrated using a fourth-order Runge-Kutta algorithm; for this purpose the four second-order differential equations, eq. 2–5, were transformed into eight first-order equations by introducing the velocities as new variables. Since the temperature of the system is defined by the temperature of the heat bath, the initial conditions are more or less arbitrary (usually $x = a/2$, $y = b$, $x_1 = -a$, $x_2 = a$, $\dot{x} = \dot{y} = \dot{x}_1 = \dot{x}_2 = 0$ were chosen as initial values). If not otherwise indicated, the time step Δt of the Runge-Kutta algorithm was $\Delta t = 0.001\ \tau_0$, where $\tau_0 \equiv a\sqrt{m_P/kT} \simeq 2$ ps. For the transmission of the random momenta to the ligands, a collision time Δt_c was defined as an integral multiple λ of the integration time step:

$$\Delta t_c = \lambda \Delta t \quad \text{(C1)}$$

In order to avoid large changes of force acting on the ligand, the momentum was not transmitted at once but stepwise (λ steps) during the collision interval Δt_c in the form of a symmetrical (ascending and descending) staircase function. For the boundary ligands λ_B was chosen to be 20, whereas

for the central ligand λ_C was varied according to the collision frequency.

In the course of the integration, it was decided for every time interval of length Δt_c (and for every individual ligand) whether or not a collision had to occur. If ν is the average collision frequency at the given instantaneous velocity of the ligand (eq. A4), then the probability that a collision occurs during Δt_c is equal to $\nu \Delta t_c$ (ν^0 and Δt_c have to be chosen such that $\nu \Delta t_c \ll 1$). A momentum was transmitted if for a random number ρ ($0 \leq \rho \leq 1$) obtained from the random number generator of the PDP11-FORTRAN library the condition $\rho < \nu \Delta t_c$ was met; otherwise the statistical force was set equal to zero during the interval Δt_c. (This procedure is based on the fact that the probability of a random number $\rho \epsilon (0, 1)$ being smaller than a given number $z \epsilon (0, 1)$ is equal to z.) If not otherwise stated, an average number of five collisions with the ligand at rest during the reference time τ_0 was assumed ($\nu^0 = 5/\tau_0$); an increase or decrease in ν^0 by a factor of two did not significantly change the results.

When a collision occurred in the interval Δt_c, the magnitude of the transmitted momentum was determined in the following way [20]. First, a random momentum $p = (2\rho - 1) p_{max}$ was selected from the interval $(-p_{max}, p_{max})$; ρ is another random number from the interval (0, 1) and $p_{max} > 0$ is a suitably chosen upper limit of the momentum (see Appendix A). With the selected momentum p the value of $h(p)$ was calculated according to eq. A8. $h(p)$ was then compared with a further random number ρ; when the condition $\rho < h(p)$ was met, the value of p was accepted, otherwise the procedure was repeated for a new value of p.

An example of a momentum distribution function obtained in this way is shown in fig. 9. Eq. A8 was written in the form (with $p^* \equiv p\sqrt{m_H / 8\mu^2 kT}$ and $c \equiv v\sqrt{m_H / 2kT}$):

$$H(p^*) = \frac{|p^*|}{p^*_{max}} \exp\left[-(c + p^*)^2\right] \qquad \text{(C2)}$$

and a large number N of random momenta p^* was generated with the distribution $H(p^*)$ for $c = 0.4$, using the random number method described above. In fig. 9 the points are the 'experimental' values of the probability density $N(p^*)/N\Delta p^*$, where $N(p^*)$ is the number of momenta lying in an interval Δp^* around p^*. The curve in fig. 9 is the theoretically expected probability density

$$F(p^*) = \frac{|p^*| \exp\left[-(c + p^*)^2\right]}{\exp(-c^2) + \sqrt{\pi}\, c \phi(c)} \qquad \text{(C3)}$$

(ϕ is the error function). Fig. 9 shows the characteristic asymmetric shape of $F(p^*)$ which results from the fact that for a positive velocity c of the ligand the transmission of a negative momentum to the ligand occurs with increased probability. This asymmetry of the momentum distribution function reflects the friction effect of the surrounding gas on the moving ligand.

References

1 S. Glasstone, K.J. Laidler and H. Eyring, The theory of rate processes (McGraw Hill, New York, 1941).
2 J.A. McCammon and M. Karplus, Annu. Rev. Phys. Chem. 31 (1980) 29.
3 T.L. Hill, Introduction to statistical thermodynamics (Addison-Wesley, Reading, 1960).
4 P. Läuger, Biophys. Chem. 15 (1982) 89.
5 W.W. Wood and J.J. Erpenbeck, Annu. Rev. Phys. Chem. 27 (1976) 319.
6 J. Kushick and B.J. Berne, in: Modern theoretical chemistry, Vol. 6, ed. B.J. Berne (Plenum Press, New York, 1977) p. 41.
7 Computer modelling of matter, ed. P. Lykos, ACS Symposium Series 86 (American Chemical Society, Washington, 1978).
8 W. Fischer, J. Brickmann and P. Läuger, Biophys. Chem. 13 (1981) 105.
9 B. Hille, J. Gen. Physiol. 58 (1971) 599.
10 B. Lassier and C. Brot, Disc. Faraday Soc. 48 (1969) 39.
11 P. Turq, F. Lantelme and H. Friedman, J. Chem. Phys. 66 (1977) 3039.
12 E. Helfand, J. Chem. Phys. 69 (1978) 1010.
13 R.M. Levy, M. Karplus and J.A. McCammon, Chem. Phys. Lett. 65 (1979) 4.
14 M.R. Pear and J.H. Weiner, J. Chem. Phys. 71 (1979) 212.
15 R.D. Present, Kinetic theory of gases (McGraw-Hill, New York, 1958).
16 J.A. McCammon, P.G. Wolynes and M. Karplus, Biochemistry 18 (1979) 927.
17 G.H.A. Cole, An introduction to the statistical theory of classical simple dense fluids (Pergamon Press, Oxford, 1967).
18 J.O. Hirschfelder, C.F. Curtiss and R.B. Bird, Molecular theory of gases and liquids (John Wiley, New York, 1954) p. 1110.

19 A.H. Stroud, Approximate calculation of multiple integrals (Prentice Hall, Englewood Cliffs, NJ, 1971).
20 J.V. Neumann, Natl. Bur. Stand. Appl. Math. Ser. 12 (1951) 36.
21 J.A. Montgomery, Jr, D. Chandler and B.J. Berne, J. Chem. Phys. 70 (1979) 4056.
22 S.A. Adelman and J.D. Doll, J. Chem. Phys. 61 (1974) 4242.
23 S.A. Adelman and J.D. Doll, J. Chem. Phys. 64 (1976) 2375.
24 D.L. Ermak and J.A. McCammon, J. Chem. Phys. 69 (1978) 1352.
25 M. Fixman, J. Chem. Phys. 69 (1978) 1527, 1538.
26 D. Beece, L. Eisenstein, H. Frauenfelder, G. Good, M.C. Marden, L. Reinisch, A.H. Reynolds, L.B. Sorensen and K.T. Yue, Biochemistry 19 (1980) 5147.